AGU PUBLICATIONS

Journal of Geophysical Research: Atmospheres

Supporting Information for

Influences of Recent Particle Formation on Southern Ocean Aerosol Variability and Low Cloud Properties

Isabel L. McCoy[1], Christopher S. Bretherton[1], Robert Wood[1], Cynthia H. Twohy[2], Andrew Gettelman[3], Charles G. Bardeen[3], and Darin W. Toohey[4]

[1] Atmospheric Sciences, University of Washington, Seattle, WA, USA, [2] Northwest Research Associates, Redmond, WA, USA, [3] National Center for Atmospheric Research, Boulder, CO, USA, [4] Atmospheric and Oceanic Sciences, University of Colorado, Boulder, CO, USA.

Contents of this file

Text S1
Caption for Movie S1
Figures S1 to S13

Additional Supporting Information (Files uploaded separately)

Movie S1

Text S1.

The instrumental setup for the CVI during SOCRATES was unique and facilitated an approximate volatility estimate. Normally, the CVI preferentially separates cloud droplets using a counterflow out the tip. For out of cloud, ambient aerosol measurements the counterflow is turned off. The CVI has two primary heaters that can affect particle volatility, one on the probe and one on the long sample line. The CVI probe was heated to ~50-60°C for the majority of the flights to evaporate water and prevent icing when sampling inside supercooled clouds. Because of the instrument and inlet configuration required on the GV, a 4.5m line heated to ~40°C was run between the inlet of the CVI and the instrument rack. The total residence time in the CVI probe and sample line is 2.3 seconds. During their passage through the heated probe and sample line, smaller, more volatile ambient aerosol particles are evaporated.

The result of this setup is that for the majority of flights during the campaign the instruments behind the CVI sampled only particles not volatile at ~50°C. During the second half of the campaign, the temperature of the CVI instrument was varied between ~25-60°C to allow for a more detailed investigation of the particle volatility observed. Since the CVI has two primary heated regions, the instrument (probe and tip) and sample line, and they behave differently when the heaters are turned off, the maximum of these three temperatures is used for estimating the volatility temperature (i.e. CVI tip, probe, and sample line). Because this analysis approach was not foreseen, the volatilization estimates produced are inexact but still useful for interpreting particle composition in the free troposphere.

Movie S1. Synoptic scale patterns influencing mid-tropospheric RPF identified air masses in the 72-hour period before sampling by RF07 (black line from Tasmania). ERA5 reanalysis maps include 700 hPa vertical velocity (colors) with a 700 hPa geopotential height contour of 2.9 km for reference (black contour). RPF trajectories (gray lines) with air mass locations (circles) colored by their altitude (white to purple, as in the ascent profiles in Figure 5a). Ascent of the first set of trajectories at ~60-hr occurs off the tip of Africa while ascent of the ~36-hr trajectories occurs off the coast of Antarctica, both driven by the advance of a warm-conveyor belt towards the south east (i.e. along the height contour).

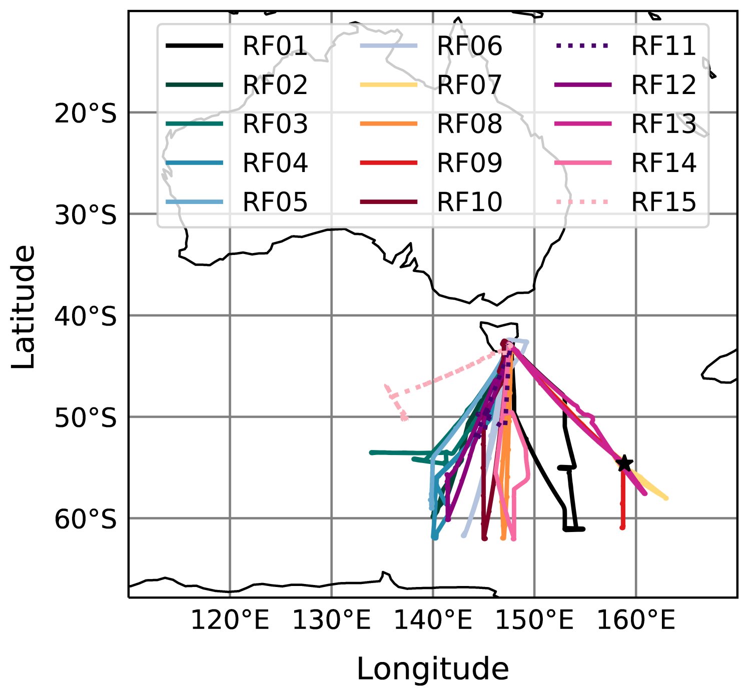

Figure S1. Research flight paths during SOCRATES (dashed lines for cumulus targeting flights, solid for standard modules). Macquarie Island, a coordinated site for ground observations as detailed in McFarquhar et al. (2020) is marked with a star.

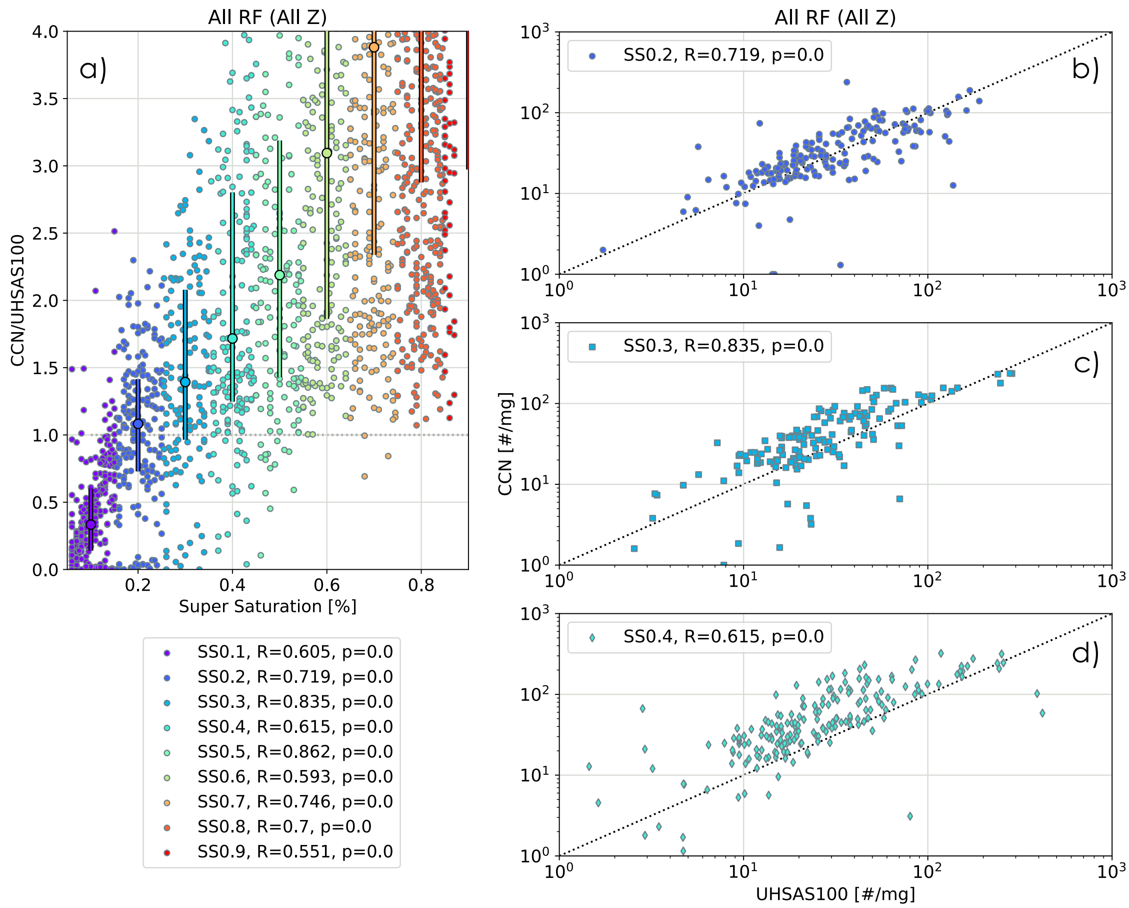

Figure S2. Relationship between scanning CCN (Sanchez & Roberts, 2018) and UHSAS100 during SOCRATES for all altitudes and samples available, binned by 1.5 minutes. (a) Ratios between CCN and UHSAS100 with correlation coefficients (legend) colored by supersaturation (SS). The three SS with ratios closest to 1 are shown separately as scatters: 0.2% (b), 0.3% (c), and 0.4% (d). SS of 0.2% is the best proxy for UHSAS100 as it has a ratio near unity and a significant correlation.

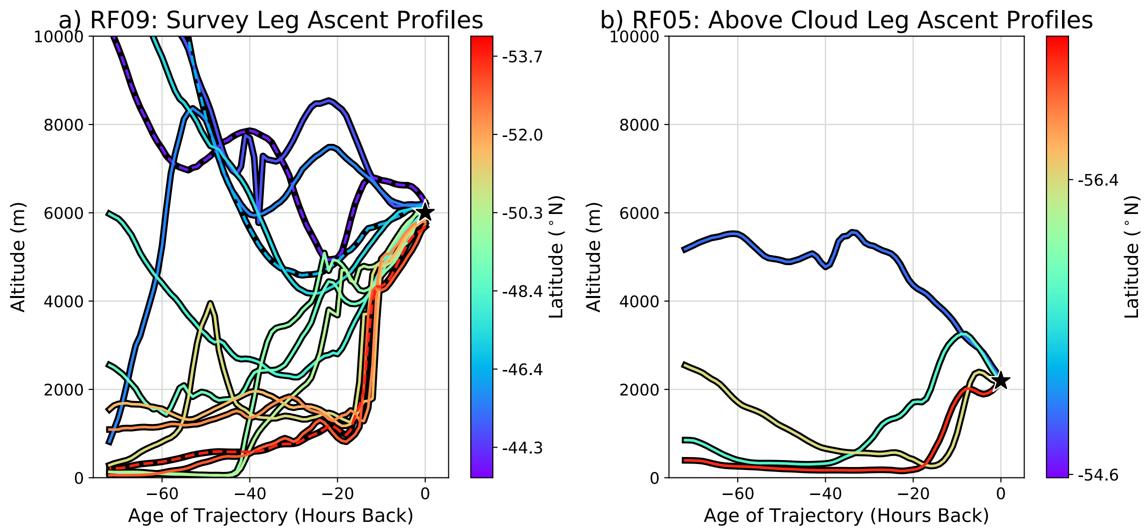

Figure S3. HYSPLIT 72-hour back trajectories of air masses initiated in 10-minute intervals corresponding to starred locations in Figure 2: (a) survey-leg sampling in the mid-troposphere during RF09, and (b) above cloud leg sampling during RF05. Lines are colored by latitude of sampled air along the GV flight path and match star locations in Figure 2. Trajectories that do not satisfy the criteria for RPF events ($CN_{Max10} < 2500$ mg^{-1}) are dashed.

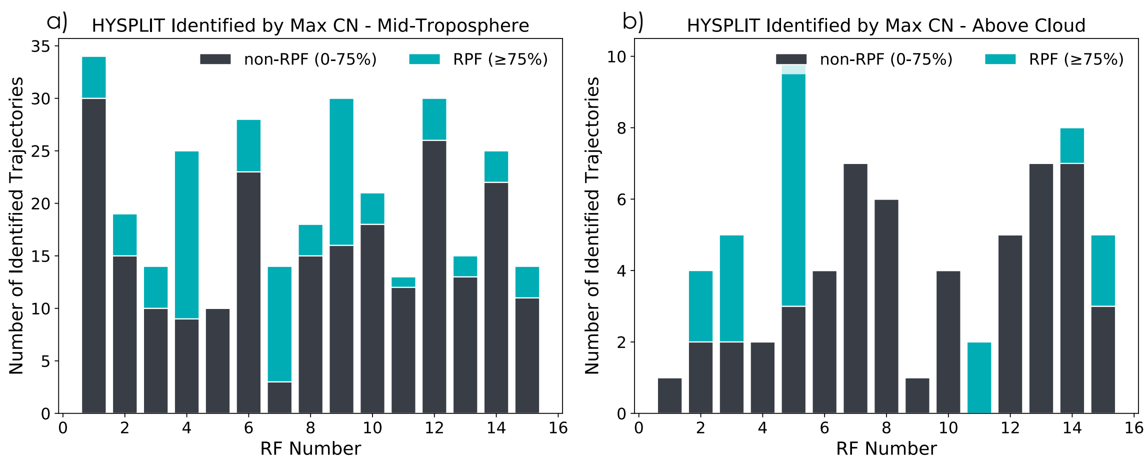

Figure S4. Number of RPF (blue) vs non-RPF identified HYSPLIT trajectories by research flight for trajectories initiated in the (a) mid-troposphere and (b) above cloud.

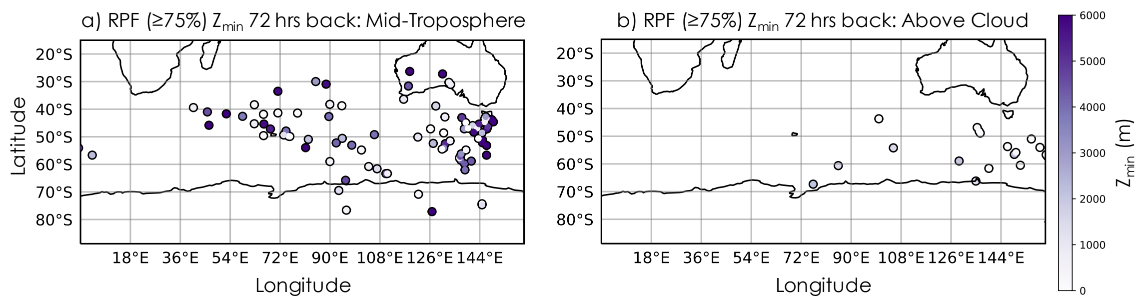

Figure S5. Location and altitude of minimum height that occurs over full 72 hours for RPF identified trajectories in (a) mid-troposphere and (b) above cloud.

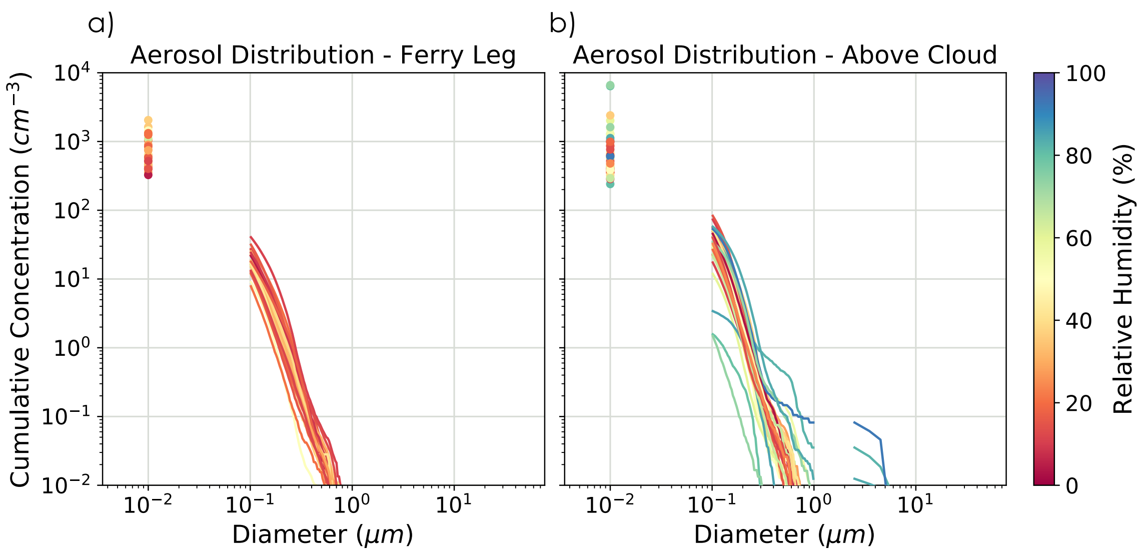

Figure S6. Median cumulative size distributions for each level leg in the mid-troposphere (a) and above cloud (b) sampled during the campaign. Each line is colored by the median relative humidity to indicate where near cloud contamination may be occurring. There are several instances of this in the above cloud sampling (b). However, the majority of the cumulative size distributions demonstrate the dominance of Aitken particles in the free troposphere (a, b). Note that concentrations are not adjusted for standard temperature and pressure.

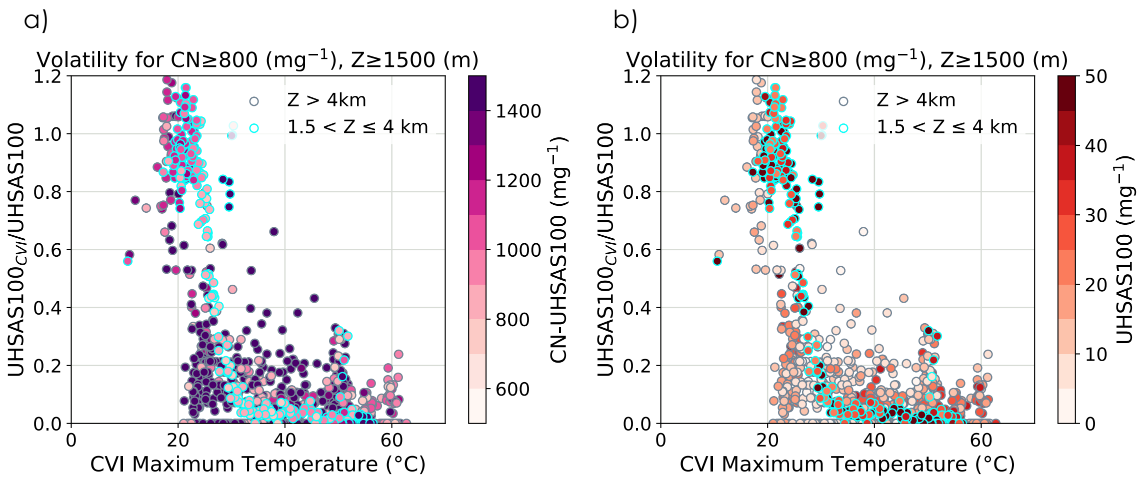

Figure S7. Volatility curves from CVI analysis as in Figure 7 but for the small number of accumulation mode particles captured in these Aitken-dominated samples. Accumulation mode volatilization is presented as the ratio between UHSAS100 and UHSAS100$_{CVI}$ versus the maximum temperature of the CVI instrument. Points are shown for CN ≥ 800 mg^{-1} and limited to free tropospheric samples (Z ≥ 1.5 km). Outline colors denote altitude of sample: mid-troposphere (gray) and above cloud (blue). Points are colored to estimate the number of particles in the Aitken mode (a, CN-UHSAS100, generally more in the mid-troposphere) and accumulation mode (b, UHSAS100, more above cloud). Note that accumulation number in these Aitken-dominated samples are rarely more than 30 mg^{-1} in mid-troposphere and increase only to ~50 mg^{-1} above cloud.

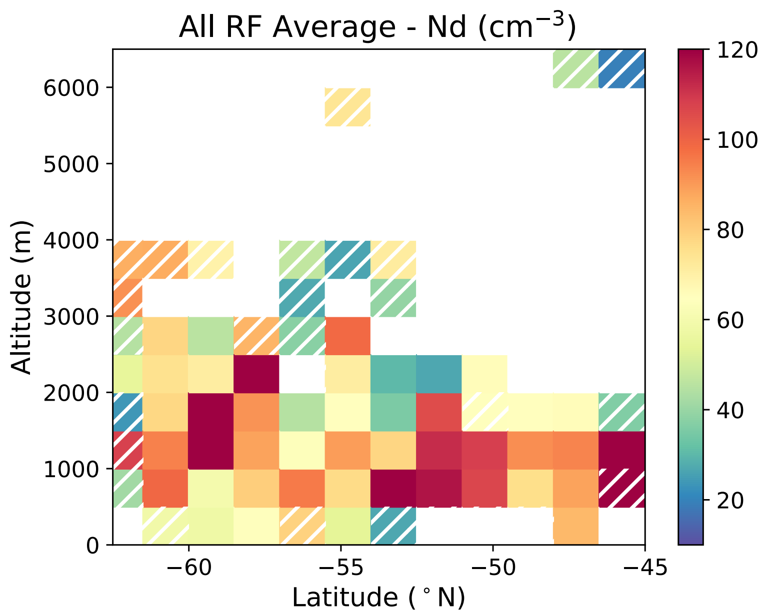

Figure S8. All flight average composite of binned flight medians (500 m x 1.5° boxes) for cloud droplet number concentration as in Figure 8d but using volume units (cm^{-3}) instead of standard temperature and pressure corrected units (mg^{-1}). Bins where 2 or less flights sampled are hatched to indicate inadequate sampling.

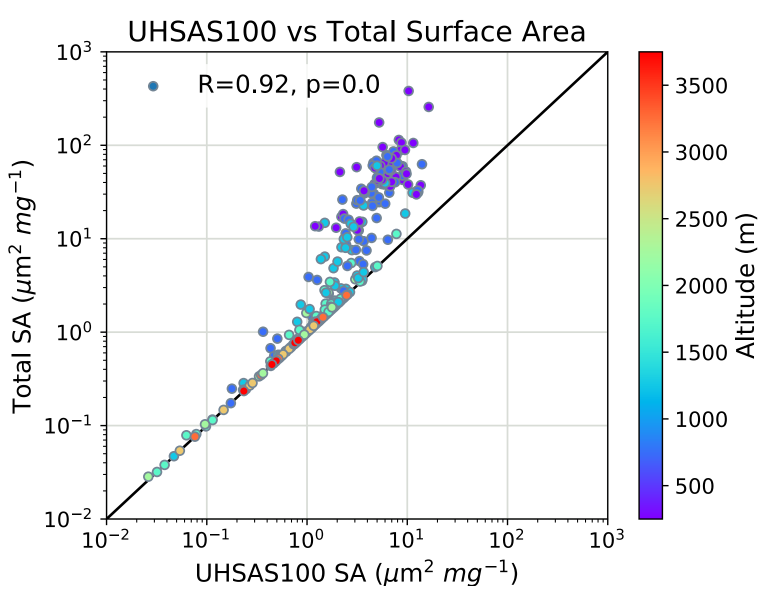

Figure S9. Total (CDP+UHSAS100) surface area vs. surface area computed from UHSAS100 alone for observations binned into 500 m x 1.5° boxes for each flight during SOCRATES. Points are colored by altitude. Only data in pristine (south of 45°S) from Z≤ 4 km are considered. A 1:1 line is included for reference along with the correlation coefficient and *p*-value for the log-log relationship.

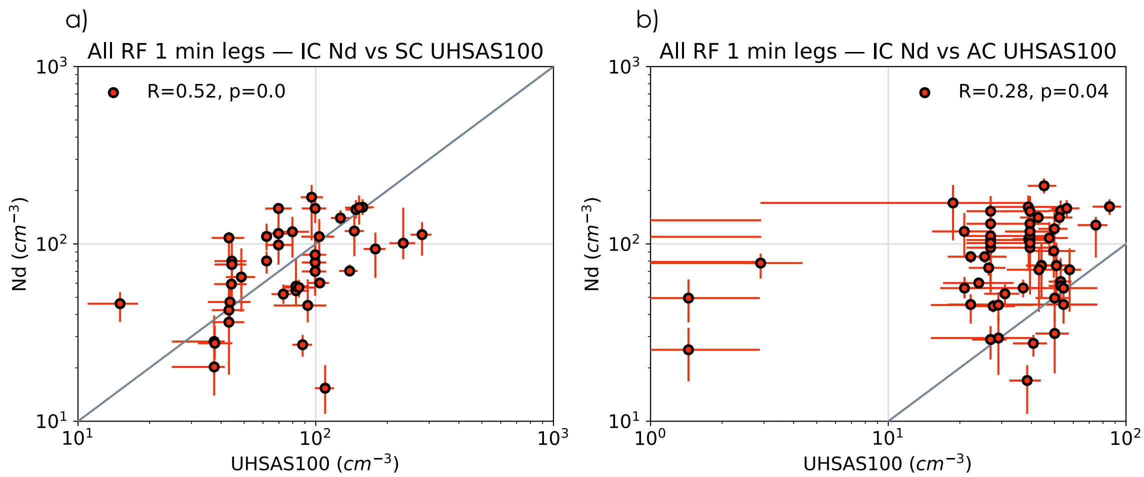

Figure S10. In-cloud median N_d versus nearest sub-cloud (a) and above-cloud (b) median UHSAS100 for SOCRATES level legs (≥1 min in length). Lines associated with each point are the 25th-75th percentiles across the level leg. A 1:1 line is included for reference as well as the correlation coefficient and p-values for each log-log relationship.

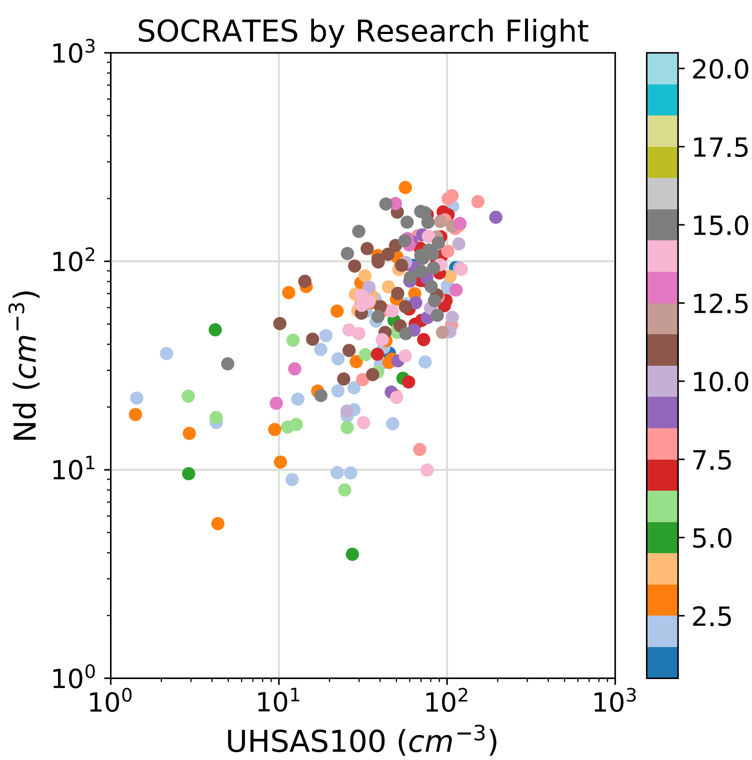

Figure S11. N_d versus UHSAS100 for SOCRATES data binned by 2 min x 50 m. Colors mark the research flight number and helps us to identify which flights have low N_d and/or low UHSAS100 occurrences.

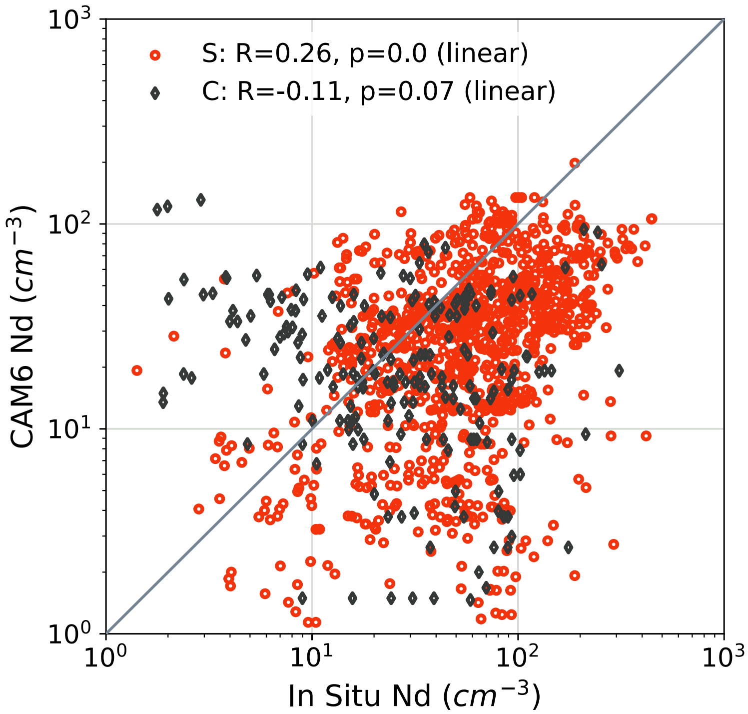

Figure S12. N_d comparison between CAM6 and in-situ samples binned by flight at 2 min x 50 m from CSET (gray) and SOCRATES (orange). A reference 1:1 line is included along with correlation coefficients and p-values computed for the linear relationship between CAM6 and observations. CAM6 over produces precipitation-depleted clouds ($N_d \leq 10$ cm^{-3}) relative to SOCRATES observations and are not collocated with actual observations for either CSET or SOCRATES.

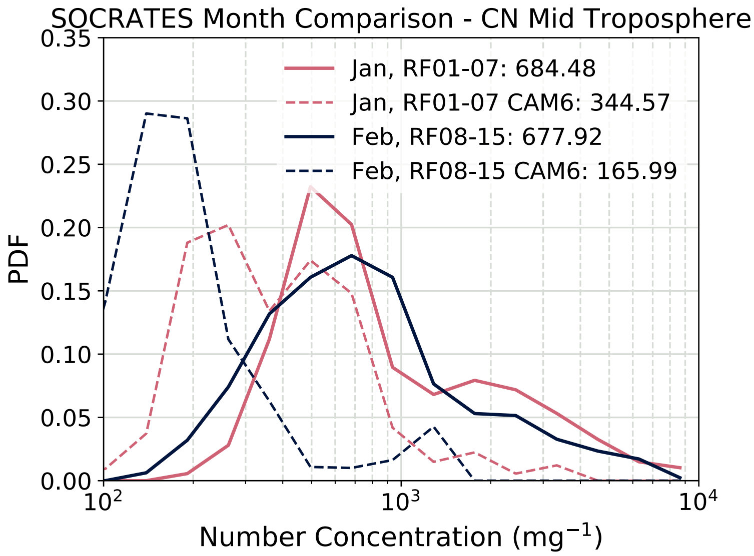

Figure S13. Observed CN number concentration in the mid-troposphere for January (RF01-07) and February (RF08-15) have similar pdfs (and similar sampling amounts), suggesting statistically consistent CN concentrations across these months. CAM6 matched CN has distinctly different PDFs for January and February, with February producing much lower CN than January and far too low relative to observations. Both CAM6 month pdfs under produce high concentrations of aerosol (CN ≥ 1000 mg^{-1}) relative to observations. Medians are provided for comparison.